Journal of Molecular and Cellular Cardiology Plus 14 (2025) 100825

Contents lists available at ScienceDirect

Journal of Molecular and Cellular Cardiology Plus

journal homepage: www.journals.elsevier.com/journal-of-molecular-andcellular-cardiology-plus

Metformin alleviates diastolic dysfunction in mice with experimental diabetic cardiomyopathy

Jordan S.F. Chan [a,b,c], Seyed Amirhossein Tabatabaei Dakhili [a,b,c], Nadeen R. Wu [a,b,c], Magnus J. Stenlund [a,b,c], Alexa N. King [a,b,c], Linyue Dong [a,b,c,d], Indiresh A. Mangra-Bala [a,b,c], Tanin Shafaati [a,b,c], Sally R. Ferrari [a,b,c], Amanda A. Greenwell [a,b,c,e], Kunyan Yang [a,b,c], Christina T. Saed [a,b,c,f], Farah Eaton [a,b,c], Keshav Gopal [a,b,c], Gregory R. Steinberg [f,h,i], Jason R.B. Dyck [b,c,g], John R. Ussher [a,b,c,*]

[a] Faculty of Pharmacy and Pharmaceutical Sciences, University of Alberta, 2-35 Medical Sciences Building, Edmonton, Alberta, T6G 2H1, Canada
[b] Alberta Diabetes Institute, University of Alberta, 112 St NW, Edmonton, Alberta, T6G 2R3, Canada
[c] Cardiovascular Research Institute, University of Alberta, Edmonton, Alberta, T6G 1C9, Canada
[d] School of Pharmacy, Shanghai University of Traditional Chinese Medicine, 1200 Cailun Road, Shanghai, 201203, China
[e] Temerty Faculty of Medicine, University of Toronto, 1 King's College Cir, Toronto, Ontario, M5S 1A8, Canada
[f] Centre for Metabolism, Obesity, Diabetes Research, McMaster University, 1280 Main St W, Hamilton, Ontario, L8S 4K1, Canada
[g] Department of Pediatrics, Faculty of Medicine and Dentistry, University of Alberta, 11405-87 Ave NW, Edmonton, Alberta, T6G 1C9, Canada
[h] Division of Endocrinology and Metabolism, Department of Medicine, McMaster University, 1200 Main St W, Hamilton, Ontario, L8N 3Z5, Canada
[i] Department of Biochemistry and Biomedical Sciences, McMaster University, 1280 Main St W, Hamilton, Ontario, L8S 4K1, Canada

ARTICLE INFO

Keywords:
Metformin
Diabetic cardiomyopathy
Obesity
Type 2 diabetes
Diastolic dysfunction

ABSTRACT

The first line therapy for managing type 2 diabetes (T2D), metformin, has been shown to be cardioprotective in humans and several preclinical models of cardiovascular disease. However, there has been limited interrogation into metformin's effects on diastolic function, a hallmark characteristic of diabetic cardiomyopathy (DbCM), which is becoming increasingly prevalent in people with pre- and early-stage T2D. Accordingly, we aimed to determine the effects of metformin on the pathogenesis of DbCM and hypothesized that treatment with metformin would alleviate diastolic dysfunction in mice with T2D. To induce experimental T2D and DbCM, male C57BL/6J mice were fed a high-fat diet for 12.5 weeks, in combination with a single, low-dose injection of streptozotocin (75 mg/kg) at week 4.5. The animals' drinking water was randomized to include either vehicle control or metformin (3.0 g/L) during the final 7.5 weeks. As expected, metformin treatment improved glycemia with a trend towards a reduction in adiposity in mice with T2D. Using ultrasound echocardiography, we observed that metformin improved diastolic function in mice with T2D as reflected by an increase and a decrease in the e′/a′ and E/e′ ratios, respectively. Furthermore, wheat-germ agglutinin staining indicated that treatment with metformin decreased cardiomyocyte hypertrophy in mice with T2D. However, mice with T2D treated with metformin did not exhibit increases in myocardial adenosine monophosphate-activated protein kinase (AMPK) phosphorylation. Thus, our findings suggest that metformin has salutary actions against DbCM and its associated diastolic dysfunction, which may be independent of its ability to increase AMPK activity.

1. Introduction

Type 2 diabetes (T2D) is a major global health crisis predominantly driven by the increasing prevalence of obesity. The International Diabetes Federation estimates that over 550 million adults are living with diabetes, the vast majority (>95 %) of which have T2D, and this number is predicted to increase to over 850 million in the next 20 years [1]. Importantly, the field has made significant advancements in the development of antidiabetic medications, and people living with T2D now have a plethora of drugs targeting unique mechanisms of action that are

* Corresponding author at: 2-020E Katz Group Centre for Pharmacy and Health Research, Faculty of Pharmacy and Pharmaceutical Sciences, University of Alberta, Edmonton, AB, T6G 2R3, Canada.
E-mail address: jussher@ualberta.ca (J.R. Ussher).

https://doi.org/10.1016/j.jmccpl.2025.100825
Received 18 June 2025; Received in revised form 26 October 2025; Accepted 12 November 2025
Available online 14 November 2025

used to manage their hyperglycemia [2]. However, even in individuals with T2D that are normotensive, asymptomatic and have well-controlled blood glucose, there is a high risk for developing macrovascular cardiovascular disease [3,4]. Furthermore, diabetic cardiomyopathy (DbCM) has been increasingly recognized in individuals with prediabetes or early-stage T2D, which is often characterized by diastolic dysfunction [5,6]. Indeed, some studies have reported that nearly 50 % of people living with T2D present with underlying diastolic dysfunction, and unfortunately there are no specific therapies available for reversing the pathology of DbCM [4]. As a result, there has been significant interest in exploring the cardiovascular actions of antidiabetic medications, especially with regards to the more recently approved therapies that include the glucagon-like peptide 1 receptor (GLP-1R) agonists and sodium glucose co-transporter 2 (SGLT2) inhibitors. While both GLP-1R agonists and SGLT2 inhibitors have been demonstrated to improve cardiovascular outcomes in people living with T2D [7,8], they have also been demonstrated in preclinical studies to alleviate diastolic dysfunction in mice with DbCM [9–11].

However, GLP-1R agonists and SGLT2 inhibitors are not first-line therapeutic options for T2D, with the initial pharmacotherapy an individual with T2D might receive after failing lifestyle interventions often being metformin. Metformin is a biguanide and first-line therapy of choice in the management of glycemia in people living with T2D [12], which induces glucose-lowering by suppressing hepatic glucose production, either via an adenosine monophosphate-activated protein kinase (AMPK)-dependent or AMPK-independent pathways [13]. Regarding the former, metformin acts by inhibiting complex I of the electron transport chain, thereby suppressing mitochondrial ATP production, activating AMPK and inhibiting hepatic gluconeogenesis. In addition to its antidiabetic actions, numerous studies have reported that metformin harbors pleiotropic benefits in the context of other diseases [14,15], including cardiovascular disease [16]. Several clinical trials, such as the UK Prospective Diabetes Study (UKPDS) and the Study on the Prognosis and Effect of Antidiabetic Drugs on Type 2 Diabetes Mellitus with Coronary Artery Disease (SPREAD-DIMCAD) demonstrated that metformin treatment is associated with a reduction for risk of myocardial infarction and major adverse cardiovascular events when compared to conventional therapy [17,18]. Metformin also appears to have salutary effects in animal models of T2D, whereby improvements in systolic function, cardiac hypertrophy and fibrosis have been observed [19–22]. These observations have largely been attributed to metformin's ability to stimulate AMPK activity in extrahepatic tissues, such as cardiomyocytes, endothelial cells and vascular smooth muscle cells.

Regarding diastolic dysfunction, compared to sulfonylurea or insulin therapy, metformin was associated with improved diastolic function as indicated by a lower isovolumetric relaxation time in an observational study of 242 diabetic patients undergoing coronary angiography [23]. Furthermore, the METformin in DIastolic Dysfunction of MEtabolic syndrome (MET-DIME) trial reported that metformin treatment on top of lifestyle counseling in nondiabetic individuals but with metabolic syndrome improved diastolic function, as reflected by an increase in e′ velocity [24]. Nevertheless, there has been limited interrogation of how metformin may impact diastolic function in both humans and animals with DbCM. Accordingly, we aimed to determine the effects of metformin treatment on diastolic function and the pathology of DbCM in an experimental mouse model reflecting the early stages of T2D. We hypothesized that treatment with a clinically relevant dose of metformin would alleviate diastolic dysfunction in mice with T2D, which would be associated with the stimulation of myocardial AMPK activity, coinciding with decreases in cardiac hypertrophy and fibrosis.

2. Material & methods

2.1. Animal care and experimentation

All animal procedures were approved by the University of Alberta Health Sciences Animal Welfare Committee and performed in accordance with the regulations of the Canadian Council on Animal Care. Animals were housed in a 22 °C temperature-controlled unit with a 12-hr light and 12-hr dark cycle, with all mice receiving standard enrichment and ad libitum access to food and water. 10–12-wk-old male C57BL/6J mice were subjected to experimental T2D/DbCM via 12.5-wks of high-fat diet (HFD) feeding (60 % from lard; Research Diets D12492) in combination with a single intraperitoneal (IP) injection of streptozotocin (STZ; 75 mg/kg) at wk. 4.5, according to previously documented guidelines [25]. Healthy, nondiabetic control mice were maintained on standard chow (PicoLab 5L0D) and instead received a single IP injection of 0.1 M citrate buffer at wk. 4.5. At wk. 5, mice were treated with either vehicle control (VC; UV-irradiated tap water) or metformin (3.0 g/L dissolved in UV-irradiated tap water) for 7.5-wks. Based on the average daily water consumption of a male C57BL/6J mouse, lean animals and animals with T2D were receiving ~600 mg/kg/day of metformin. This dose was selected as it has previously been shown to elicit clinically relevant serum concentrations of metformin [26,27]. Body weight and ad libitum blood glucose was monitored bi-weekly. At study completion, animals were subjected to a 4-hr fast, 1-hr refeed via oral gavage of Ensure prior to being euthanized by an IP injection of sodium pentobarbital (12 mg). Tissues (e.g. heart, liver, kidneys) were extracted, snapped-frozen using liquid N_2-cooled Wollenberger tongs and stored at −80 °C for further molecular interrogation.

2.2. Assessment of in vivo cardiac function

Transthoracic ultrasound echocardiography was performed using a VisualSonics Vevo 3100 rodent ultrasound imaging system and images were acquired with a MX550S probe, as previously described [10,28]. In brief, mice were anaesthetized using 1.5–3.0 % isoflurane, after which their chest were shaved and ultrasound transmission gel was applied. Heart rate, respiratory rate, body temperature and electrophysiology were continuously monitored throughout the image acquisition process. Echocardiography images acquired from animals with heart rates <350 beats per min (bpm) or >450 bpm were excluded from the study. Echocardiography was performed prior to and following VC or metformin treatment. To obtain a complete assessment of LV systolic and diastolic function as well as LV structure, several parameters were acquired including mitral pulse wave E/A ratio, tissue Doppler e′/a′ ratio, E/e′ ratio, % LV ejection fraction and LV wall dimensions. Echocardiography images were analyzed using VisualSonics Vevo Lab 5.7.1.

2.3. Enzyme-linked immunosorbent assay

To measure circulating growth differentiation factor (GDF15) levels, tail blood was collected at study completion from mice with T2D treated for 7.5-wks with VC or metformin. Blood samples were centrifuged at 2000 ×*g* for 20 min at 4 °C, following which the supernatant (plasma) was collected and quantified for GDF15 levels using a mouse GDF15 enzyme-linked immunosorbent assay kit (RDR-GDF15-Mu, Reddot Biotech), according to the manufacturer's instructions.

2.4. Glucose and insulin tolerance testing

At 4-wks post-treatment, animals were subjected to an IP glucose tolerance test to assess glucose homeostasis. Mice were administered a bolus of glucose (1 g/kg) following a 16-hr fast, and tail blood was sampled for the measurement of blood glucose levels using the Contour Next blood glucose monitoring system (Bayer) at 0-, 15-, 30-, 60-, 90- and 120-min post-glucose injection. An IP insulin tolerance test was also performed at 5-wks post-treatment to measure insulin sensitivity. Animals were given a single IP injection of insulin (0.7 U/kg) following a 6-hr fast, and blood glucose levels were quantified at 0-, 15-, 30-, 60-, 90- and 120-min post-insulin administration.

2.5. H9C2 cardiac myoblast cultures

H9C2 rat cardiac myoblasts (ATCC CRL-1446) were cultured in Dulbecco's Modified Eagle Medium (DMEM; Gibco 2764658) supplemented with 10 % fetal bovine serum (v/v) (Gibco 16000044) and 1 % penicillin-streptomycin (v/v) (Gibco 15140122) at 37 °C in a humidified 5 % CO_2 (v/v) atmosphere. Cells were trypsinized and passaged every 2–3 days or before they reached 80 % confluency.

2.6. Immunoblotting

Frozen myocardial tissue (~10 mg) was powdered using a liquid N_2-cooled pestle and mortar and homogenized using a TissueLyser II (Qiagen) in 300 μL of lysis buffer containing 50 mM Tris HCl (pH 8 at 4 °C), 1 mM ethylenediaminetetraacetic acid, 10 % glycerol (w/v) and 0.02 % Brij-35 (w/v), 1 mM dithiothreitol, 0.5 mM of sodium orthovanadate (Na_3VO_4), 2.5 mM of sodium fluoride and protease and phosphatase inhibitors (Sigma Aldrich). Samples were centrifuged at 21,100 ×*g* for 20 min at 4 °C and the resulting supernatant was collected and quantified for protein concentration using the Bradford method, following which western blotting was performed as previously described [28]. In brief, 30 μg of protein sample was prepared in sodium dodecyl sulfate (SDS) sample buffer, heated at 95 °C for 5 min and loaded in a 12 % polyacrylamide gel. Gels were subjected to SDS-PAGE (Sodium Dodecyl Sulfate Polyacrylamide Gel Electrophoresis) and subsequently transferred to a nitrocellulose membrane. Membranes were blocked in 5 % milk and incubated overnight in primary antibody at 4 °C. Phospho-acetyl CoA carboxylase (ACC) serine 79 (11818S; Cell Signaling Technology), ACC (3662S; Cell Signaling Technology), phospho-AMPK threonine 172 (2535S; Cell Signaling Technology), AMPK (5831S; Cell Signaling Technology), phospho-endothelial nitric oxide synthase (eNOS) serine 1177 (9570T; Cell Signaling Technology), eNOS (3207T; Cell Signaling Technology), microtubule-associated proteins 1A/1B light chain 3B (LC3B) (3868S; Cell Signaling Technology), O-linked *N*-acetylglucosamine (O-GlcNAc) (9875T; Cell Signaling Technology), parkin (2132S; Cell Signaling Technology), phosphatase and tensin homolog-induced kinase 1 (PINK1) (ab23707; Abcam), pyruvate dehydrogenase (PDH) kinase 4 (PDK4) (AP7041B; Abgent), phospho-PDH serine 232 (AP1063; Millipore Sigma) and phospho-PDH serine 300 (AP1064; Millipore Sigma), PDH (3205S; Cell Signaling) primary antibodies were prepared in 1:1000 dilution in 3 % bovine serum albumin (BSA) with 0.02 % NaN_3. Anti-mouse (7076S; Cell Signaling Technology) or anti-rabbit (7074S; Cell Signaling Technology) secondary antibodies were prepared in a 1:2000 dilution in 5 % milk. Afterwards, membranes were incubated in secondary antibodies for 1.5 h at room temperature and luminesced using Clarity Western Enhanced Chemiluminescence Substrate (BioRad). Analysis and densitometry was performed using Bio-Rad Image Lab software.

2.7. Immunohistochemistry and immunofluorescence

Animals were euthanized with sodium pentobarbital (12 mg) at study completion and hearts were arrested in diastole through an apical injection of 1 M KCl into the LV. To exsanguinate the animal, a small excision was made in the right atrium and 10 mL of sterile PBS was perfused via a 21-gauge needle inserted into the apex of the LV. Afterwards, the LV was perfused with 10 mL zinc-buffered formalin (StatLab 195205) and excised for further processing. Hearts were subsequently embedded in paraffin, sectioned at 5–6 μm and stained with picrosirius red to assess LV interstitial and perivascular fibrosis. In addition, staining with Oregon Green 488-conjugated wheat-germ agglutinin (WGA; #W11261, Thermo Fisher Scientific) and 4′,6-diamidino2-phenyllindole (DAPI; D3571, Thermo Fisher Scientific) was also performed to determine LV cardiomyocyte size.

To measure NFκB nuclear translocation, H9C2 cells were fixed with 4 % paraformaldehyde for 15 min and then permeabilized with 0.5 % Triton X-100 in PBS/0.1 % Tween-20 (v/v) for 10 min at room temperature. Afterwards, cells were blocked with 3 % BSA for 1 h and incubated with anti-NFκB (8242S; Cell Signaling Technology) overnight at 4 °C. Cells were subsequently washed with PBS/0.1 % Tween-20 (v/v) and incubated with a CoraLite488-conjugated anti-rabbit secondary antibody (SA00013-2; Proteintech) in PBS for 1 h, stained with DAPI and mounted with Elvanol antifade reagent.

To assess cross-sectional area, H9C2 cells were grown on coverslips in a 6-well plate and co-treated with metformin (5 μM, 10 μM) and lipopolysaccharide (LPS; 1 μg/mL) for 1 h. Following treatment, cells were fixed in buffered zinc formalin for 10 min at 37 °C. Cells were then incubated with Oregon Green 488-conjugated WGA (#W11261, Thermo Fisher Scientific) at 50 μg/mL for 10 min at room temperature. Afterwards, cells were permeabilized with 0.2 % Triton X-100 in PBS for 3 min at room temperature and then counterstained with DAPI (D3571, Thermo Fisher Scientific). Between each incubation, slides were washed 3 times with 1 mL of PBS. Coverslips were mounted on slides using a Elvanol antifade reagent, and an Axio Observer.A1 inverted fluorescence microscope (Zeiss) was used to visualize the cells and to acquire images for immunohistochemistry and immunofluorescence, which were quantified using ImageJ.

2.8. Magnetic resonance imaging

Total lean and fat mass were quantified using an EchoMRI-4in1/700 body composition analyzer via quantitative nuclear magnetic resonance relaxometry in lean mice and mice with T2D prior to and following metformin treatment.

2.9. 3-[4,5-Dimethylthiazol-2-yl]-2,5 diphenyl tetrazolium bromide (MTT) assay

To measure cell viability, H9C2 cells were transferred to 96-well plates and co-treated with metformin (5 μM, 10 μM) and lipopolysaccharide (LPS; 1 μg/mL) for 1 h. Immediately following treatment, cells were incubated in a 0.5 mg/mL MTT (475989-1GM, Millipore) solution diluted in serum-free cell culture media for 4 h. After incubation, the MTT solution was aspirated and the remaining formazan produced was solubilized in 200 μL of DMSO, following which cell viability was assessed by measuring the absorbance at 570 nm.

2.10. Quantitative real-time PCR

To isolate RNA, powdered frozen heart tissue (~10 mg) was homogenized in 1.0 mL of TRIzol (Invitrogen 520812) using a TissueLyser II (Qiagen), following which 200 μL of chloroform was added and samples were centrifuged at 14,000 ×*g* for 10 min at 4 °C. The aqueous layer was collected and added to 500 μL of ice-cold isopropanol. Samples were centrifuged at 16,000 x*g* for 10 min at 4 °C and washed once with 1 mL of ice-cold 75 % EtOH. Pellets were left to air-dry for 30 min and resuspended in 30 μL of RNase-free water. RNA concentration was determined using a NanoDrop 2000 spectrophotometer. A High-Capacity cDNA Reverse Transcription Kit (Applied Biosystems 4368814) was used to synthesize first strand complementary DNA (cDNA) from 2 μg of RNA according to the manufacturer's instructions. Real-time PCR using various primers for several genes (Supplemental Table 1) was performed on cDNA samples with the CFX Connect Real-time PCR machine (BioRad) and the $2^{-\Delta\Delta Ct}$ method [29] was used to quantify relative mRNA transcript levels with peptidylprolyl isomerase A (*Ppia*) as a housekeeping gene.

2.11. Triacylglycerol (TAG) isolation and quantification

TAGs was isolated and quantified from the hearts of mice with T2D treated with VC or metformin as previously described [10]. Briefly, powdered frozen myocardial tissue (~15 mg) was homogenized in 40 μL

of a 2:1 chloroform:methanol solution and centrifuged at 3,500 rpm for 10 min at 4 °C. 80 μL of 0.04 % $CaCl_2$ was added to the supernatant, centrifuged at 2400 rpm for 20 min at 4 °C and the resulting upper phase was removed. The interface was rinsed 3 times with 150 μL pure solvent upper phase, following which 50 μL of methanol was added and dried under N_2 at 60 °C. TAGs was redissolved in 50 μL 3:2 tert-butyl alcohol: Triton X-100 and quantified using an enzymatic assay kit (Wako Pure Chemical Industries) per the manufacturer's instructions.

2.12. Statistical analysis

All values are presented as mean ± standard error of the mean (SEM). Unpaired, nonparametric 2-tailed Mann-Whitney *U* tests were used to determine statistical significance between two groups. A one-way analysis of variance (ANOVA) followed by a Bonferroni post-hoc analysis was used when an experimental outcome was influenced by one experimental variable. A repeated measures two-way ANOVA or a two-way ANOVA test followed by a Bonferroni post-hoc analysis was used when an experimental outcome was influenced by two experimental variables. No data were considered outliers by testing or were arbitrarily excluded. Differences were considered significant if $P < 0.05$.

3. Results

3.1. Metformin treatment improves glucose tolerance in mice with T2D

10–12-wk-old male C57BL/6J mice were maintained on standard chow (lean controls) or subjected to an experimental model of T2D via 12.5-wks of HFD feeding in combination with a single, low-dose STZ injection at wk. 4.5. At wk. 5, animals were treated with either vehicle control (VC; UV-irradiated tap water) or metformin (3.0 g/L dissolved in UV-irradiated tap water) for 7.5-wks (Fig. 1A). As expected, mice with T2D demonstrated significant weight gain which was accompanied by an increase in % fat mass and a decrease in % lean mass relative to healthy, nondiabetic controls (Fig. 1B–D). Metformin treatment did not cause any changes in body composition in either lean mice or mice with T2D (Fig. 1B–D), although there was a trend towards a decrease in

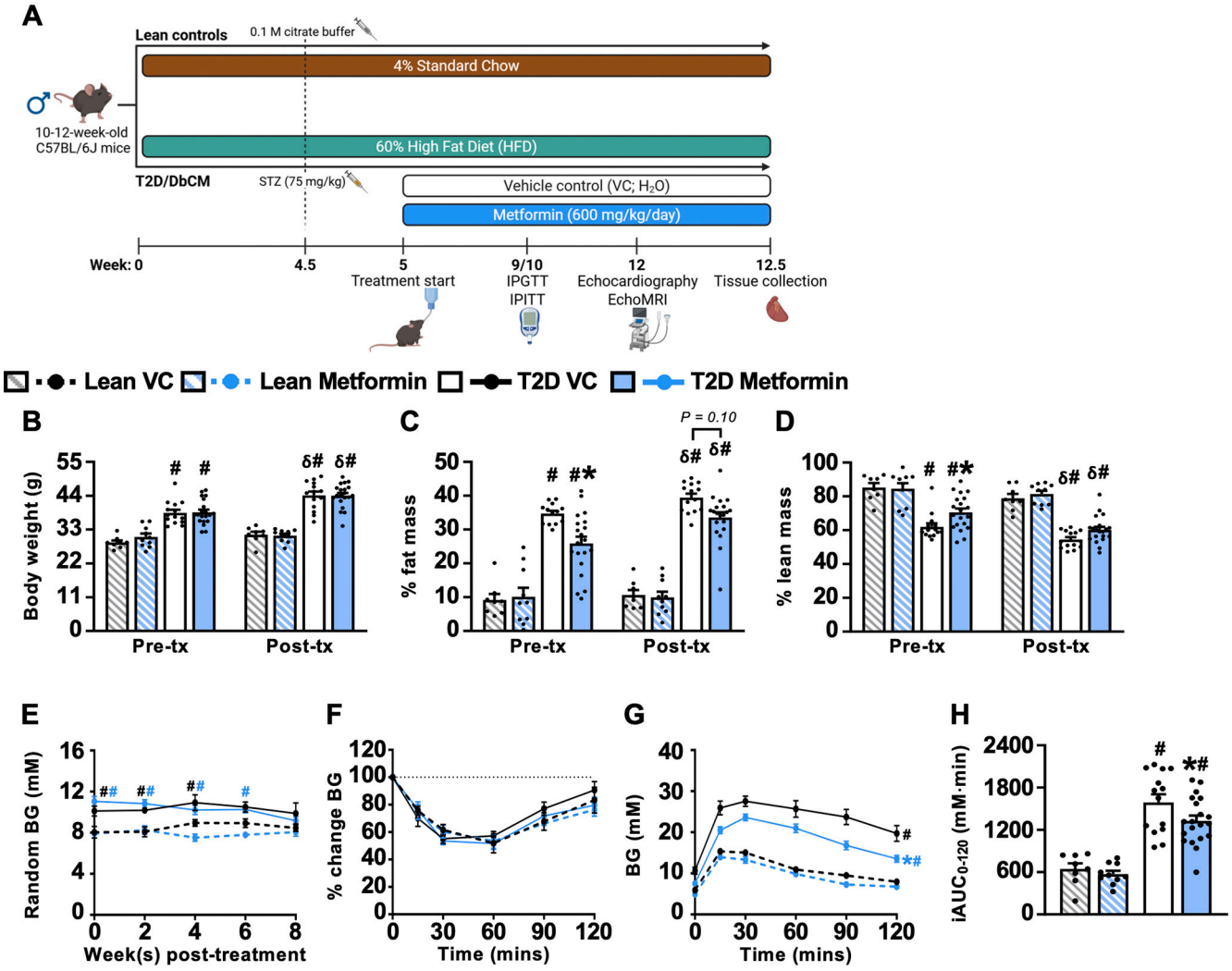

Fig. 1. Metformin treatment improves glucose tolerance in mice with T2D. (A) Schematic representation of the experimental design used for the in vivo animal studies. (B) Body weight, (C) % fat mass and (D) % lean mass in lean mice and mice with T2D before and after 7.5-wks of treatment with either vehicle control (VC) or metformin ($n = 8–20$ mice/group). (E) Ad-libitum blood glucose measured bi-weekly in lean mice and mice with T2D treated with VC or metformin for 7.5-wks (n = 8–20 mice/group). (F) Intraperitoneal insulin tolerance test, (G) intraperitoneal glucose tolerance test and (H) the associated integrated area under the curve (iAUC) in lean mice and mice with T2D at 4–5 weeks post-VC or metformin treatment (n = 8–20 mice/group). The iAUC was calculated using the fasting glycemia value as the baseline. Values represent mean ± SEM. Differences were determined using a repeated measures two-way ANOVA (B–G) or a two-way ANOVA (H) followed by a Bonferroni post-hoc analysis. $^{*}P < 0.05$, significantly different versus respective VC counterpart. $^{\#}P < 0.05$, significantly different versus respective lean counterpart. $^{\delta}P < 0.05$, significantly different versus respective pre-treatment counterpart.

adiposity in mice with T2D treated with metformin compared to their VC treated counterparts (Fig. 1C). In addition, treatment with metformin had no effect on ad libitum blood glucose or insulin sensitivity in mice with T2D (Fig. 1E,F) but led to an improvement in glucose tolerance (Fig. 1G,H).

3.2. Metformin alleviates left ventricular diastolic dysfunction without altering systolic function in mice with T2D

Compared to healthy nondiabetic controls, mice with experimental T2D developed diastolic dysfunction as evidenced by a decreased mitral Tissue Doppler e′/a′ ratio, increased E/e′ ratio and prolonged isovolumetric relaxation time (IVRT) but preserved LV systolic function (Supplemental Table 2). This is consistent with our previous reports [28,30] and recapitulates the cardiac phenotype observed in humans with DbCM [5]. Using ultrasound echocardiography, we observed that although 7.5-wks of metformin treatment did not affect the mitral E/A ratio, it led to an improvement in other parameters of diastolic dysfunction, reflected by an increase and a decrease in the e′/a′ and E/e′ ratios, respectively (Fig. 2A–H). Surprisingly, treatment with metformin increased both the % LV ejection fraction (LVEF) and % LV fractional shortening (LVFS) in lean mice, which may be attributed to a few VC treated lean mice having lower systolic function than what is generally observed, although this was not recapitulated in mice with T2D (Fig. 2I–L). Furthermore, other parameters of systolic function such as cardiac output were unaltered by T2D or treatment with metformin (Fig. 3D and Supplemental Table 2).

3.3. Metformin decreases cardiomyocyte size in mice with T2D

Mice with experimental DbCM developed a mild cardiac hypertrophy as seen by a thickening of the LV anterior wall during diastole (Fig. 3A). Metformin treatment in mice with T2D did not impact LV anterior/posterior wall thickness or LV internal diameter but did result in a mild increase in LV mass and LV mass normalized to lean body mass (Fig. 3A–D). In contrast, histological assessment of LV cross-sections stained with wheat-germ agglutinin revealed that metformin treatment reduced cardiomyocyte size in mice with T2D (Fig. 3E,F). This was associated with a significant reduction in smooth muscle α-2 actin (*Acta2*) and a trend towards a decrease in myocardial atrial natriuretic peptide (*Nppa*) mRNA expression, whereas mRNA expression of other markers of cardiac hypertrophy such as brain natriuretic peptide (*Nppb*) and myosin heavy chain 7 (*Myh7*) were unchanged (Fig. 3G).

3.4. Treatment with metformin did not increase myocardial AMPK or eNOS phosphorylation

Metformin has been widely reported to elicit cardioprotection via

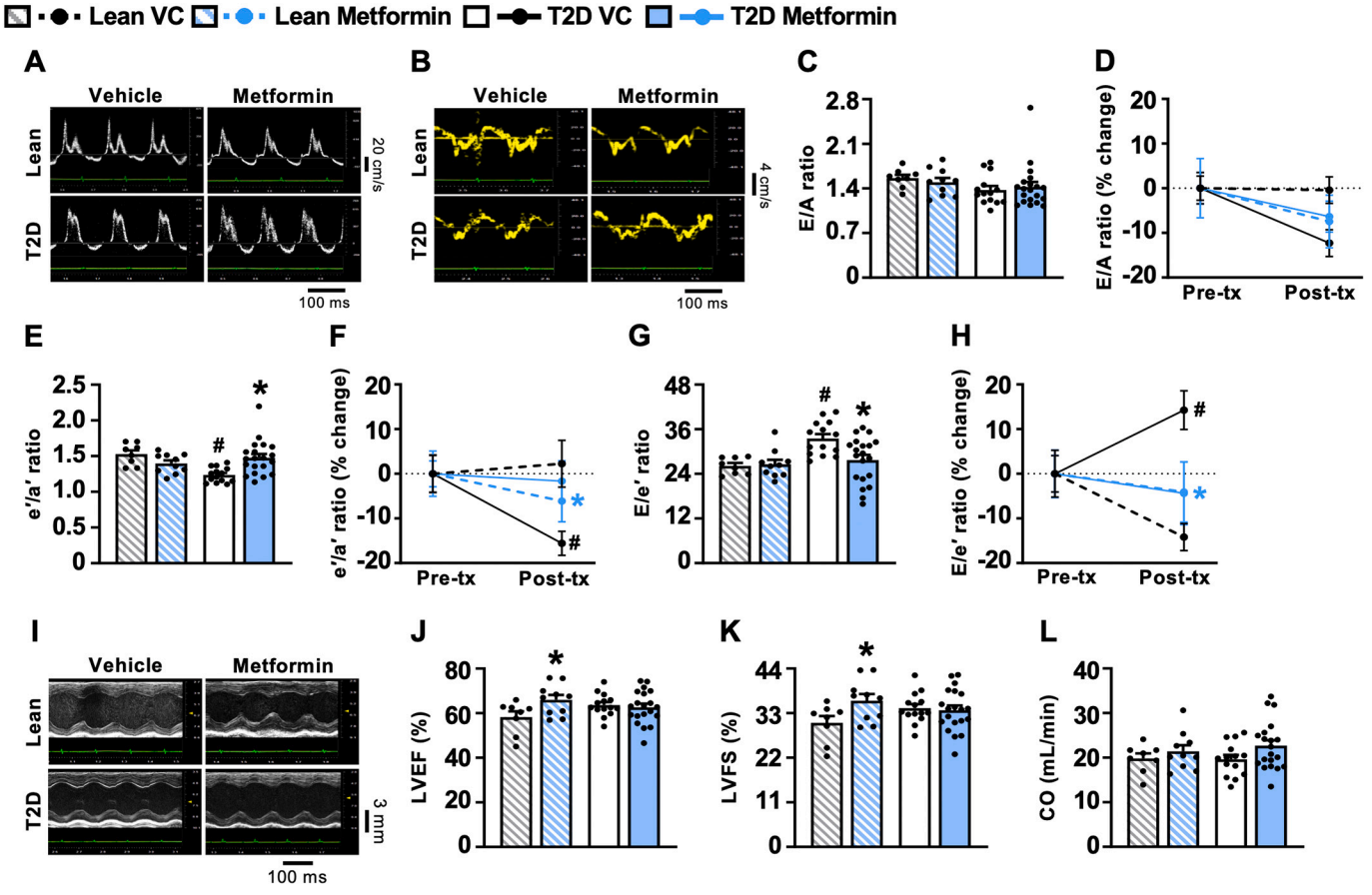

Fig. 2. Metformin alleviates left ventricular diastolic dysfunction without affecting systolic function in mice with T2D.
(A) Representative images of pulse-wave Doppler, (B) representative images of tissue Doppler, (C) mitral E/A ratio, (D) percent change in mitral E/A ratio after treatment, (E) mitral e′/a′ ratio, (F) percent change in mitral e′/a′ ratio after treatment, (G) E/e′ ratio, (H) percent change in mitral E/e′ ratio after treatment, (I) Representative M-mode images, (J) percent left ventricular (LV) ejection fraction (LVEF), (K) percent fractional shortening (LVFS) and (L) cardiac output (CO) assessed using ultrasound echocardiography in lean mice and mice with T2D mice after a 7.5-wk treatment with either vehicle control (VC) or metformin (n = 8–20 mice/group). Values represent mean ± SEM. Differences were determined using a two-way ANOVA (C, E, G, J–L) or a repeated measures two-way ANOVA (D, F, H) followed by a Bonferroni post-hoc analysis. $^{*}P < 0.05$, significantly different versus respective VC counterpart. $^{\#}P < 0.05$, significantly different versus respective lean counterpart.

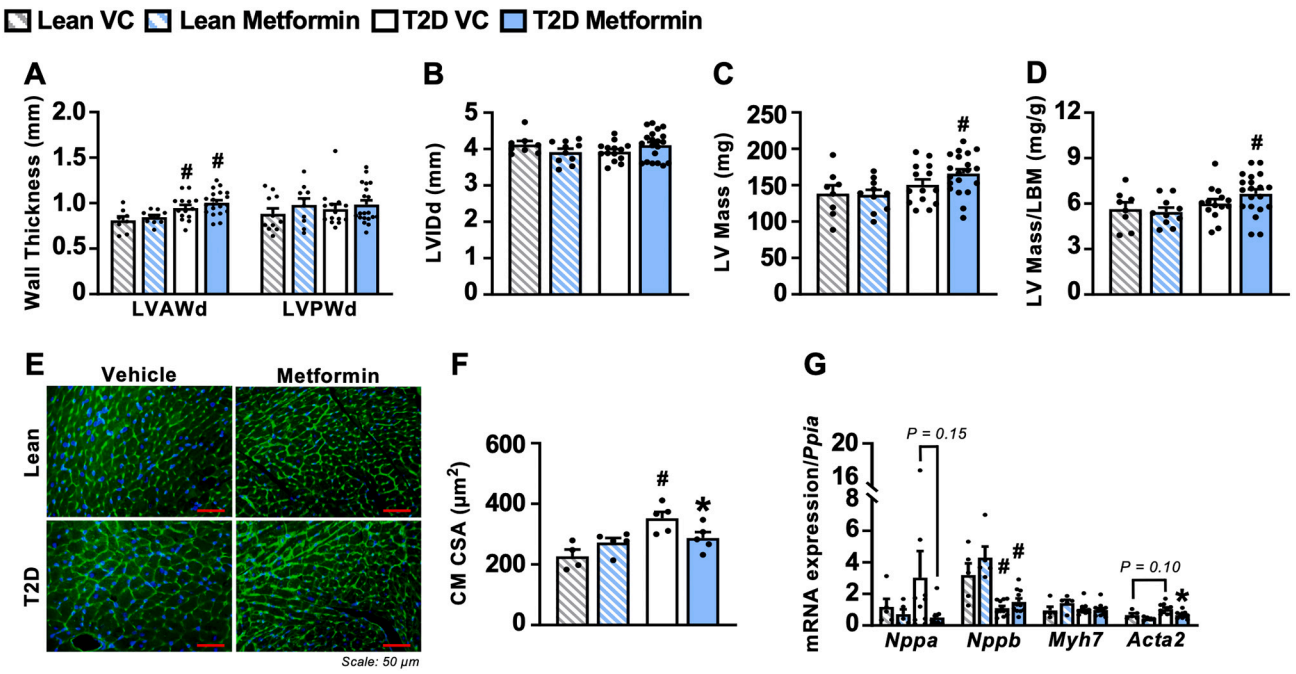

Fig. 3. Metformin treatment decreased cardiomyocyte size but not wall thickness in mice with T2D. (A) Left ventricular (LV) anterior wall thickness during diastole (LVAWd) and LV posterior wall thickness during diastole (LVPWd), (B) LV internal diameter during diastole (LVIDd), (C) LV mass and (D) LV mass normalized to lean body mass (LBM) as assessed by ultrasound echocardiography in lean mice and mice with T2D 7.5-wks after treatment with vehicle control (VC) or metformin (n = 8–20 mice/group). (E) Representative images of wheat germ agglutinin staining of LV sections and (F) LV cardiomyocyte (CM) cross-sectional area (CSA) in lean mice and mice with T2D following treatment with either VC or metformin for 7.5-wks (n = average of 15 cardiomyocytes from 4 to 5 mice/group). Scale bar, 50 μm. (G) Relative mRNA expression of biomarkers for cardiac hypertrophy (*Nppa*, *Nppb*, *Myh7* and *Acta2*) normalized to *Ppia* mRNA expression in myocardial extracts of lean mice and mice with T2D at 7.5-wks post-treatment (n = average of 3 technical replicates from 5 to 11 mice/group). Values represent mean ± SEM. Differences were determined using a two-way ANOVA (A–D, F–G) followed by a Bonferroni post-hoc analysis. $^{*}P < 0.05$, significantly different versus respective VC counterpart. $^{\#}P < 0.05$, significantly different versus respective lean counterpart. *Acta2*, smooth muscle α-2 actin; *Myh7*, myosin heavy chain 7; *Nppa*, atrial natriuretic peptide; *Nppb*, brain natriuretic peptide; *Ppia*, peptidylprolyl isomerase A.

stimulating AMPK activity in cardiomyocytes [21,31,32]. Because AMPK phosphorylation at threonine-172 is often reflective of AMPK activity, we measured myocardial AMPK threonine-172 phosphorylation, which was unaffected in mice with T2D treated with metformin (Supplemental Fig. 1A). In addition, we also observed no changes in myocardial acetyl CoA carboxylase serine 79 phosphorylation, a downstream target of AMPK signaling (Supplemental Fig. 1B). Likewise, others have also reported that metformin can increase eNOS phosphorylation and/or activity [33], hence we also interrogated whether metformin may impact eNOS status, though metformin treatment exhibited no discernable effect on myocardial eNOS phosphorylation in mice with T2D (Supplemental Fig. 2). This suggests that the beneficial actions of metformin in our study may be independent of both AMPK and eNOS.

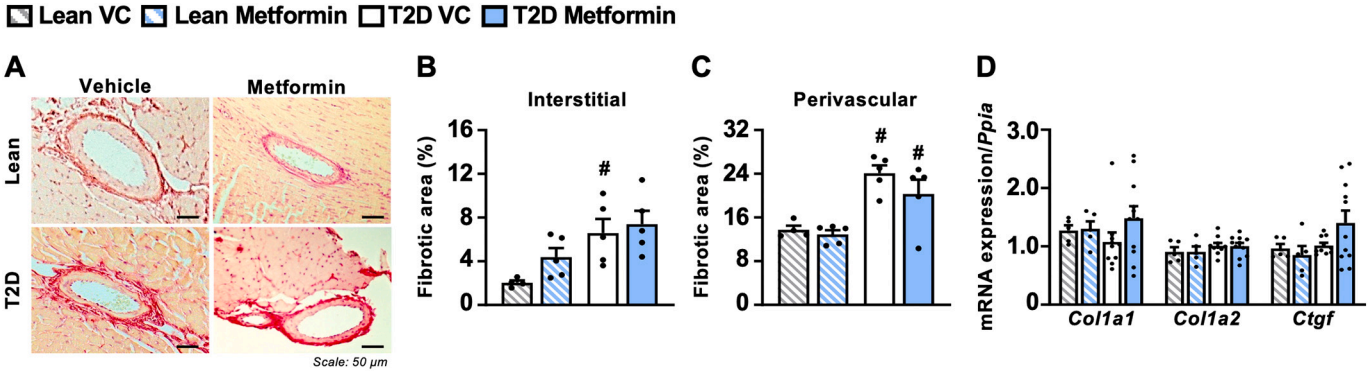

Fig. 4. Myocardial fibrosis was unchanged with metformin treatment in mice with T2D.
(A) Representative images of picrosirius red staining of the left ventricular (LV) myocardium, (B) percent LV interstitial fibrotic area and (C) percent LV perivascular fibrotic area in lean mice and mice with T2D following a 7.5-wk treatment with vehicle control (VC) or metformin (n = average of 3 LV sections from 4 to 5 animals/group). Scale bar, 50 μm. (D) Relative myocardial mRNA expression of key regulators of fibrosis (*Col1a1, Col1a2,* and *Ctgf*) normalized to *Ppia* mRNA expression in lean mice and mice with T2D treated with VC or metformin for 7.5-wks (n = average of 3 technical replicates from 5 to 11 mice/group). Values represent mean ± SEM. Differences were determined using a two-way ANOVA (B–D) followed by a Bonferroni post-hoc analysis. $^{*}P < 0.05$, significantly different versus respective VC counterpart. $^{\#}P < 0.05$, significantly different versus respective lean counterpart. *Col1a1,* collagen type 1 alpha 1; *Col1a2,* collagen type 1 alpha 2; *Ctgf*, connective tissue growth factor; *Ppia*, peptidylprolyl isomerase A.

3.5. Metformin treatment did not impact other mediators of DbCM pathology

Next, we interrogated several mediators that are implicated in the pathology of DbCM. To assess myocardial fibrosis, we performed picrosirius red staining on LV cross-sections to measure interstitial and perivascular fibrosis, both of which were not reduced with metformin treatment in mice with T2D (Fig. 4A–C). In further support of these observations, myocardial mRNA expression of key regulators involved in extracellular matrix and fibrotic deposition such as collagen type 1 alpha 1 (*Col1a1*), collagen type 1 alpha 2 (*Col1a2*), and connective tissue growth factor (*Ctgf*) were not decreased with metformin treatment in mice with T2D (Fig. 4D).

As DbCM is characterized by several perturbations in myocardial substrate metabolism [34], namely reductions and elevations in myocardial glucose and fatty acid oxidation respectively, we next measured myocardial expression of key enzymes involved in the regulation of these metabolic pathways. Of interest, metformin treatment in T2D mice led to mild increases in the myocardial mRNA expression of PDK4 (*Pdk4*) and hexokinase 2 (*Hk2*) (Fig. 5A); however, further interrogation revealed that metformin did not elicit any changes in PDK4 protein expression or PDH phosphorylation (Fig. 5B–D). Similarly,

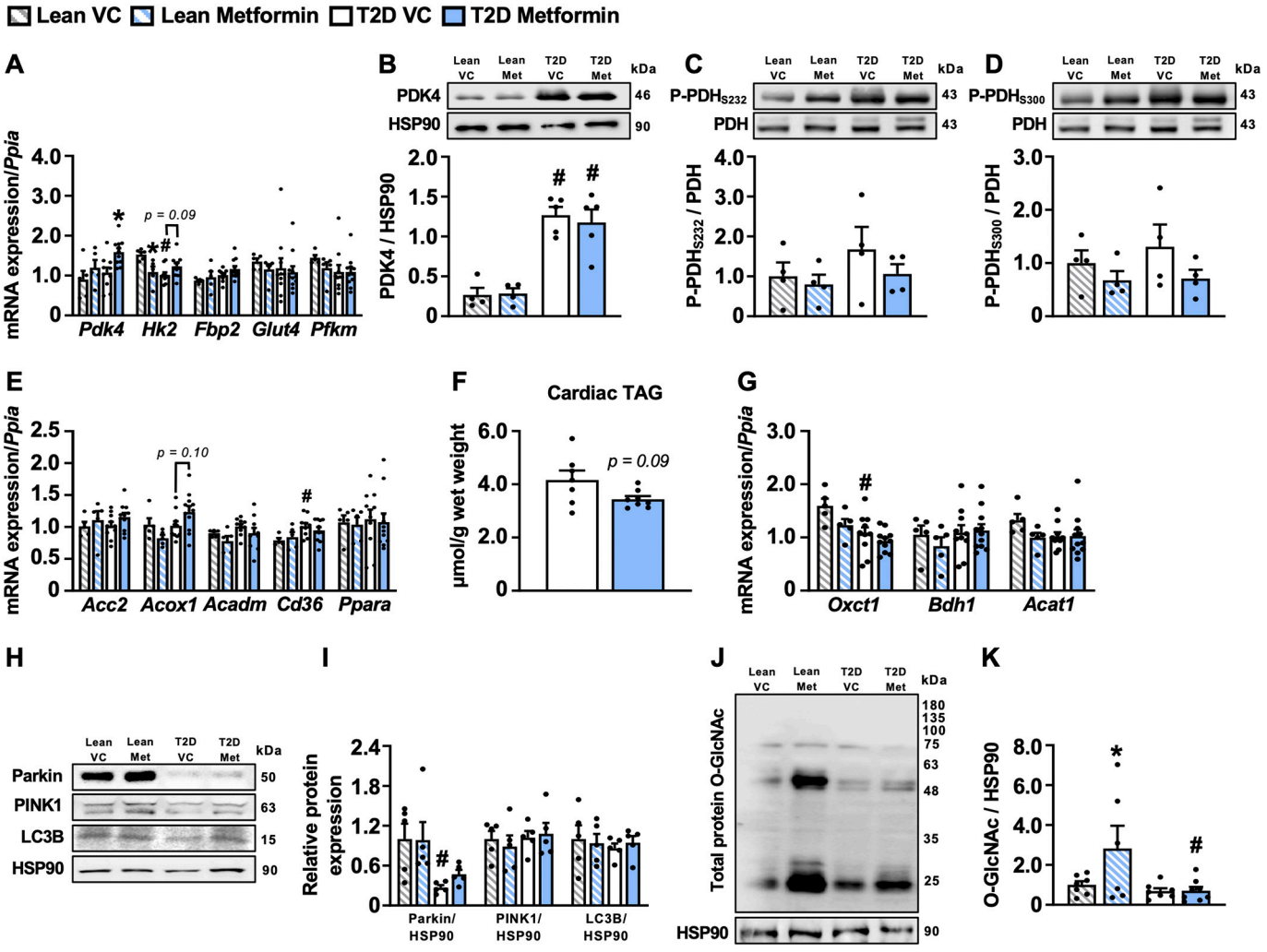

Fig. 5. Metformin treatment did not alter myocardial substrate metabolism in mice with T2D.
(A) Relative myocardial mRNA expression of key enzymes involved in glucose metabolism (*Pdk4, Hk2, Fbp2, Glut4* and *Pfkm*) normalized to *Ppia* mRNA expression in lean mice and mice with T2D treated with vehicle control (VC) or metformin for 7.5 weeks (n = average of 3 technical replicates from 5 to 11 mice/group). (B) Protein expression of PDK4, (C) PDH phosphorylation at serine 232 and (D) serine 300 in myocardial extracts from lean mice and mice with T2D at 7.5-wks post-treatment (n = 4–5 samples/group). (E) Relative myocardial mRNA expression of key regulators of fatty acid metabolism (*Acc2, Acox1, Acadm, Cd36* and *Ppara*) normalized to *Ppia* mRNA expression in lean mice and mice with T2D after 7.5-wks treatment with VC or metformin (n = average of 3 technical replications from 5 to 11 mice/group). (F) TAG content in myocardial extracts from mice with T2D at 7.5-wks post-treatment (n = 7–8 samples/group). (G) Relative myocardial mRNA expression of key enzymes involved in ketone metabolism (*Oxct1*, *Bdh1* and *Acat1*) normalized to *Ppia* mRNA expression. (H, I) Representative western blot images and densitometry for parkin, PINK1 and LC3B, and (J, K) representative western blot images and total protein O-GlcNAc levels in myocardial extracts of lean mice and mice with T2D 7.5-wks post-treatment (n = average of 3 technical replicates from 5 to 11 samples/group for qPCR data; n = 5–8 samples/group for western blot data). Values represent mean ± SEM. Differences were determined using a two-way ANOVA (A–E, G, I, K) followed by a Bonferroni post-hoc analysis or an unpaired, 2-tailed non-parametric Mann-Whitney U test (F). $^{*}P < 0.05$, significantly different versus respective VC counterpart. $^{\#}P < 0.05$, significantly different versus respective lean counterpart. *Acadm,* acyl-CoA dehydrogenase medium chain; *Acat1*, acetyl-CoA acetyltransferase; *Acc2*, acetyl-CoA carboxylase 2; *Acox1,* acyl-CoA oxidase 1; *Bdh1,* 3-hydroxybutyrate dehydrogenase 1; *Cd36*, cluster of differentiation 36; *Fbp2,* fructose bisphosphatase 2; *Glut4*, glucose transporter type 4; *Hk2,* hexokinase 2; HSP90, heat shock protein 90; LC3B, microtubule-associated proteins 1A/1B light chain 3B; O-GlcNAc, O-linked *N*-acetylglucosamine; *Oxct1*, 3-oxoacid CoA-transferase 1; PINK1, phosphatase and tensin homolog-induced kinase 1; PDH, pyruvate dehydrogenase; PDK4/*Pdk4*, pyruvate dehydrogenase kinase 4; *Pfkm*, phosphofructokinase muscle; *Ppara*, peroxisome proliferator activated receptor alpha; *Ppia*, peptidylprolyl isomerase A; TAG, triacylglycerol.

metformin treatment in mice with T2D did not alter myocardial mRNA expression of several enzymes involved in myocardial fatty acid metabolism, with the exception of a mild increase in acyl CoA oxidase 1 (*Acox1*) (Fig. 5E). Interestingly, myocardial TAG content was mildly decreased in mice with T2D following treatment with metformin, suggesting a reduction in myocardial lipid accumulation and potential lipotoxicity (Fig. 5F). As ketone metabolism has also been implicated in DbCM [35,36], we also measured myocardial mRNA expression of several ketolytic enzymes, all of which were unchanged in response to metformin treatment in mice with T2D (Fig. 5G).

In parallel with impairments in myocardial substrate metabolism, DbCM is also characterized by mitochondrial dysfunction, in part due to alterations in mitophagy [37]. Given previous evidence suggesting that metformin can impact autophagy/mitophagy [38,39], we next assessed whether metformin treatment altered the myocardial expression of key proteins involved in these regulatory pathways. Surprisingly, metformin did not increase the protein expression of parkin, PINK1 or microtubule-associated proteins 1A/1B light chain 3B (LC3B) in the hearts of mice with T2D (Fig. 5H–I).

As metformin treatment improved overall glucose homeostasis in our model, we posited that reductions in myocardial O-GlcNAcylation could contribute to metformin-mediated improvements in diastolic dysfunction in DbCM. However, experimental T2D did not impact myocardial O-GlcNAc levels, which were unaffected via treatment with metformin, though we did observe increases in myocardial O-GlcNAc levels in lean mice treated with metformin (Fig. 5J,K).

Lastly, we assessed whether metformin elicits its protective actions via attenuating myocardial inflammation. A 7.5-wk metformin

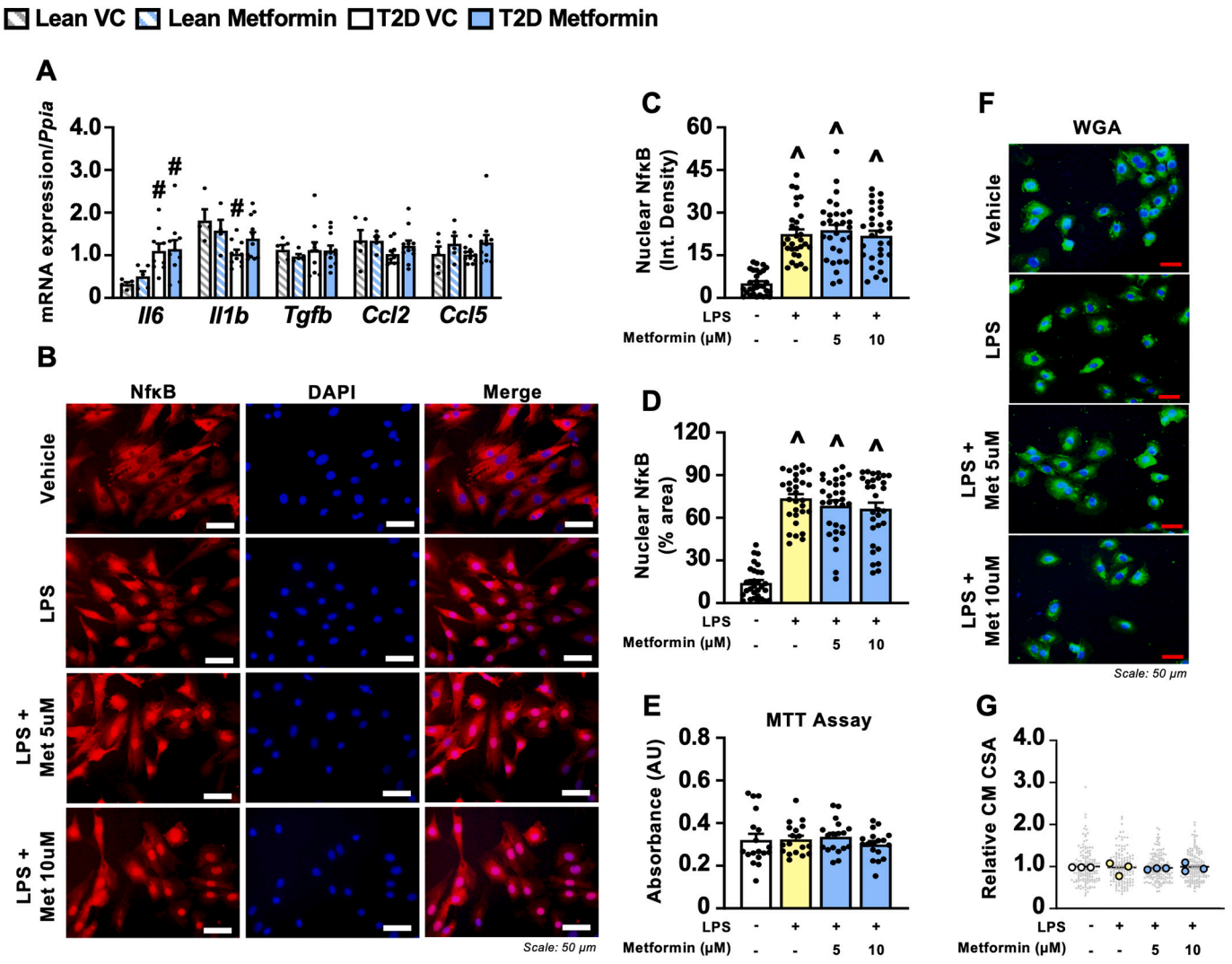

Fig. 6. Metformin treatment does not attenuate inflammation in mice with T2D or H9C2 cardiac myoblasts. (A) Relative mRNA expression of pro-inflammatory cytokines (*Il6*, *Il1b* and *Tgfb*) and chemokines (*Ccl2* and *Ccl5*) normalized to *Ppia* mRNA expression in myocardial extracts of lean mice and mice with T2D following a 7.5-wk treatment with vehicle control (VC) or metformin (n = average of 3 technical replicates from 5 to 11 mice/group). (B) Representative immunofluorescence images of H9C2 cells stained with nuclear factor κ B (NFκB) and 4′,6-diamidino-2-phenylindole (DAPI) (C) Integrated density of NFκB (n = average of 10 myoblasts from 3 biological replicates), (D) percent nuclear area of NFκB expression (n = average of 10 myoblasts from 3 biological replicates), (E) cell viability determined via MTT assay (n = average of 6 technical replicates from 3 biological replicates/group), (F) representative immunofluorescence images of H9C2 cells stained with WGA and DAPI and (G) relative cardiomyocyte (CM) cross-sectional area (CSA) (n = average of 35–60 cardiac myoblasts from 3 biological replicates/group), following a 1-hr incubation with either vehicle (sterile PBS) or lipopolysaccharide (LPS; 1 μg/mL) with or without metformin (5 or 10 μM) (Scale bar, 50 μm). Values represent mean ± SEM. Differences were determined using a two-way ANOVA followed by a Bonferroni post-hoc analysis (A) or a one-way ANOVA followed by a Bonferroni post-hoc analysis (C–E, G). $^{\#}P < 0.05$, significantly different versus respective lean counterpart. $^{\wedge}P < 0.05$, significantly different versus VC-treated H9C2 cells. *Ccl2,* chemokine ligand 2; *Ccl5,* chemokine ligand 5; *Il1b*, interleukin 1b; *Il6,* interleukin 6; *Ppia*, peptidylprolyl isomerase A; *Tgfb*, transforming growth factor B.

treatment did not alter the myocardial mRNA expression of several proinflammatory cytokines (*Il6, Il1b* and *Tgfb*) and chemokines (*Ccl2* and *Ccl5*) in mice with T2D (Fig. 6A). As several other studies have reported that metformin can reduce inflammation in cardiomyocytes [40–42], we further assessed its anti-inflammatory actions in vitro using H9C2 rat cardiac myoblasts. Consistent with our aforementioned observations in whole heart lysates from mice with T2D, metformin treatment (5–10 μM) of H9C2 cells failed to decrease LPS-induced NFκB translocation (Fig. 6B–D). Furthermore, cell viability using an MTT assay (Fig. 6E) nor cell size via WGA staining (Fig. 6F–G) were affected via LPS treatment alone or in combination with metformin.

4. Discussion

Our findings demonstrate that treatment with a clinically relevant dose of metformin is cardioprotective, as it improved several parameters of diastolic function in male mice subjected to experimental T2D/DbCM. In addition, metformin treatment decreased cardiomyocyte size but failed to improve other mediators of DbCM including myocardial energetics, fibrosis and inflammation. Surprisingly, the myocardial actions of metformin appear to be independent of its ability to stimulate AMPK activity, as myocardial AMPK phosphorylation was unchanged in response to treatment with metformin.

One of the key pathological changes that occur in the myocardium during the progression of DbCM is the excessive accumulation of collagen and fibrotic tissue [43], which consequently impairs LV compliance and diastolic function. Our model of DbCM recapitulates these characteristics as evidenced by increases in both LV interstitial and perivascular fibrosis when assessed via picrosirius red staining. However, we did not observe any reductions in myocardial fibrosis nor were there any changes in the myocardial mRNA expression of key fibrotic markers in mice with T2D treated with metformin. This was unexpected as several studies have reported that metformin treatment produces an antifibrotic effect in animal models of DbCM. For example, male Wistar rats with T2D induced by a high-carbohydrate, HFD and low-dose STZ showed significant protection against cardiac fibrosis following metformin administration [22,44]. Similarly, metformin treatment in male C57BL/6J mice subjected to STZ-induced T1D exhibited lower myocardial interstitial fibrosis as measured by Masson's trichrome staining [20,45]. These discrepancies are unclear but could be partly explained by differences in the duration of metformin treatment. While our metformin treatment only lasted 7.5 wks, the aforementioned studies employed much longer treatment periods at a similar dose, ranging from 12 to 16 wks, with some studies also including a 2-wk pre-treatment period prior to diabetes induction. In contrast, studies in Zucker diabetic fatty rats administered metformin (300 mg/kg/day mixed into the diet) for a similar duration as our study (7.5-wks) also did not observe any differences in cardiac fibrosis [46].

We also observed that treatment with metformin appeared to have no discernible effect on markers of either myocardial inflammation or substrate metabolism. The latter was particularly surprising, given that metformin has been well documented to stimulate the activity of AMPK, a central regulator of energy metabolism [47]. However, metformin's ability to alleviate diastolic dysfunction in mice with experimental DbCM appears to be independent of increased AMPK activity, as mice with T2D treated with metformin in our study did not exhibit increases in myocardial AMPK phosphorylation or phosphorylation of the AMPK-regulated downstream target, ACC. We reason this was likely due to the route of administration, as previous studies administering metformin to mice in the drinking water at the same dose resulted in metformin concentrations ranging from ~3–10 μM [27], whereas in vitro metformin concentrations in the mM range are often required to activate AMPK. It should also be noted that we did not actually measure AMPK enzymatic activity or complex I activity in our study, the latter of which has been proposed to account for how metformin stimulates AMPK activity [48]. Nonetheless, many studies have shown strong correlation between AMPK threonine 172 phosphorylation and AMPK activity [48,49]. As such, our findings clash with many other studies that have attributed the cardioprotective actions of metformin to increases in AMPK activity. For instance, in mice subjected to experimental myocardial infarction via 60-min temporary left anterior descending coronary artery occlusion followed by reperfusion, the addition of metformin (125 μg/kg) at the time of reperfusion in combination with once daily IP metformin injections for 4-wks significantly improved LVEF and preserved LV wall dimensions [33]. These effects were attributed to metformin's ability to increase myocardial AMPK and eNOS activity, as genetic knockout of either gene resulted in the loss of metformin-mediated cardioprotection [33], though metformin also did not affect eNOS status in our study. Similar findings were observed in a murine model of T1D-associated DbCM, as treatment with metformin (200 mg/kg/day via drinking water) ameliorated LV systolic dysfunction and nucleotide-binding domain, leucine-rich-containing family, pyrin domain-containing-3 expression via an AMPK-dependent pathway [21]. It remains possible that these discrepancies can be explained by metformin's inability to stimulate myocardial AMPK activity in our study, and such that only when metformin stimulates myocardial AMPK activity would one observe favourable actions on myocardial inflammation, fibrosis and/or substrate metabolism. In further relation to the former, it should also be noted that we only explored mRNA expression of inflammatory markers in myocardial extracts, and whether metformin may impact other aspects of inflammation (e.g. immune cell infiltration into the myocardium) is unknown.

The question thus remains as to how metformin improved diastolic function in mice with T2D in our study. Of interest, others have previously shown that metformin treatment can stimulate GDF15 secretion and circulating GDF15 levels in obese mice fed a HFD [27,50]. Moreover, we have recently reported that treatment with recombinant GDF15 can alleviate diastolic dysfunction and prevent the progression of experimental DbCM [28]. However, we do not believe that increases in GDF15 secretion and GDF15-mediated signaling can explain our observations as we saw no differences in circulating GDF15 levels in mice with T2D treated with metformin in comparison to their VC treated counterparts (Supplemental Fig. 3).

Taken together, the exact molecular mechanism through which metformin mitigates diastolic dysfunction in T2D remains unknown in our study. We posit that these salutary actions may be indirectly mediated via the general metabolic benefit we observed following treatment with metformin, which led to mild reductions in overall adiposity while also improving glucose homeostasis. Regarding the latter, prolonged exposure to high blood glucose levels can cause unwanted post-translational modifications (PTMs) of important proteins in the heart, such as O-GlcNAcylation [51] and glycosylation [52]. Of relevance, accumulation of these intermediates has been shown to be detrimental and can contribute to the pathogenesis of DbCM [53,54], while preventing these PTMs can significantly improve cardiac function [55,56]. Despite evidence suggesting that metformin treatment (50 μM) can alleviate global O-GlcNAcylation in primary adult mouse cardiomyocytes exposed to high glucose [57], we observed no effect on total myocardial O-GlcNAc levels following metformin treatment in mice with T2D. Likewise, whether attenuation of glycosylation may explain the benefits of metformin in DbCM was not investigated in our study and will need to be considered in future studies, as others have reported that metformin treatment (1.0 g/kg/day) reduced collagen glycosylation and improved diastolic chamber stiffness in canines with alloxan-induced diabetes [58].

Because we observed a decrease in cardiomyocyte size, another possible contributor towards metformin-mediated cardioprotection may relate to its anti-hypertrophic actions, which has also been reported by several groups in other models of cardiovascular disease [59–61]. Furthermore, experimental T2D increased myocardial *Nppa* expression, compatible with increases in atrial natriuretic peptide secretion in response to mechanical stress, whereas others have demonstrated that

atrial natriuretic peptide may have direct pro-hypertrophic actions on cardiomyocytes [62]. As metformin treatment decreased myocardial *Nppa* expression in mice with T2D, this may contribute to how metformin alleviates cardiac hypertrophy. On the contrary, these observations are incompatible with the lack of reduction in LV wall thickness and the increased LV mass we observed in mice with T2D treated with metformin. While these discrepancies cannot easily be reconciled, it is important to note that measurements of LV mass using M-mode ultrasound echocardiography have several limitations (e.g. assumptions on 3D LV geometry) that need to be considered [63].

One of the major limitations of this study is that our experiments were conducted only in male animals even though there are apparent sex differences in both the incidence and pathology of DbCM [64]. As such, further investigation will be required to determine whether metformin is protective against DbCM in female mice, though it is important to note that female mice do not develop overt diastolic dysfunction using the HFD/low-dose STZ model of T2D [25]. Another caveat of our study is that metformin was administered prior to the onset of DbCM, and that our model of T2D is more reflective of humans with early-stage T2D [25]. Since metformin is the first line therapy for humans living with T2D [12], while there is increasing evidence that humans with early-stage T2D often have an undiagnosed and asymptomatic diastolic dysfunction [5,34,65], we rationalized that early treatment would be more translationally relevant. However, it will also be important to assess whether metformin can reverse established diastolic dysfunction and DbCM in experimental models that are more reflective of humans with late-stage T2D. Lastly, the mechanism(s) through which metformin alleviates diastolic dysfunction in T2D are not fully understood and additional investigation is necessary. We aim to address this in future studies with omics-based and RNA sequencing approaches in hearts of mice treated with metformin, and validated using insulin resistant human induced pluripotent stem cell-derived cardiomyocytes [66], a more translational in vitro model versus the H9c2 cells used in the current study.

In summary, a clinically relevant dose of metformin alleviates diastolic dysfunction in mice with experimental DbCM. While the mechanisms responsible for these salutary actions are unknown, they appear to be independent of increased myocardial AMPK activity. Given the increasing recognition that individuals with early-stage T2D often have diastolic dysfunction, our findings add further support for the use of metformin in these individuals, since metformin is the first-line therapy that many of these individuals would receive as their initial pharmacotherapy for T2D.

CRediT authorship contribution statement

Jordan S.F. Chan: Writing – review & editing, Writing – original draft, Visualization, Validation, Methodology, Investigation, Formal analysis, Data curation, Conceptualization. **Seyed Amirhossein Tabatabaei Dakhili:** Writing – review & editing, Visualization, Methodology, Investigation, Data curation, Conceptualization. **Nadeen R. Wu:** Writing – review & editing, Visualization, Investigation, Formal analysis, Data curation. **Magnus J. Stenlund:** Writing – review & editing, Validation, Investigation, Data curation. **Alexa N. King:** Investigation, Validation, Writing – review & editing. **Linyue Dong:** Writing – review & editing, Validation, Investigation. **Indiresh A. Mangra-Bala:** Writing – review & editing, Validation, Investigation. **Tanin Shafaati:** Writing – review & editing, Validation, Investigation. **Sally R. Ferrari:** Writing – review & editing, Investigation. **Amanda A. Greenwell:** Writing – review & editing, Investigation. **Kunyan Yang:** Writing – review & editing, Investigation. **Christina T. Saed:** Writing – review & editing, Investigation. **Farah Eaton:** Writing – review & editing, Investigation. **Keshav Gopal:** Writing – review & editing, Methodology, Investigation, Conceptualization. **Gregory R. Steinberg:** Writing – review & editing, Conceptualization. **Jason R.B. Dyck:** Writing – review & editing, Resources. **John R. Ussher:** Writing – review & editing, Writing – original draft, Visualization, Supervision, Resources, Project administration, Methodology, Funding acquisition, Data curation, Conceptualization.

Declaration of Generative AI and AI-assisted technologies in the writing process

The authors did not use any AI-assisted technology for the preparation of this work.

Sources of funding

J.R.U. is supported by a Tier 2 Canada Research Chair in Pharmacotherapy of Energy Metabolism in Obesity. G.R.S. is supported by a Diabetes Canada Investigator Award (DI-5-17-5302-GS), a Canadian Institutes of Health Research (CIHR) Foundation Grant (201709FDN-CEBA-116200), a Tier 1 Canada Research Chair in Metabolic Diseases, and a J. Bruce Duncan Endowed Chair in Metabolic Diseases. J.R.B.D. is supported by a Canada Research Chair in Molecular Medicine and received funding from the CIHR, the Heart and Stroke Foundation of Canada, and Diabetes Canada. J.S.F.C. is supported by a Canada Graduate Scholarship – Doctoral from the CIHR. S.A.T.D. is supported by a Postdoctoral Fellowship from the CIHR. I.A.M is supported by a Canada Graduate Scholarship – Master's from the CIHR. A.A.G. is supported by a Vanier Canada Graduate Scholarship from the CIHR.

Declaration of competing interest

G.R.S. has received research funding through McMaster University from Esperion Therapeutics, Nestle, Merck, Cambrian Biosciences, Novo Nordisk, Poxel Pharmaceuticals and Espervita Therapeutics; honoraria and/or consulting fees from Astra Zeneca, Cambrian Biosciences, Eli-Lilly, Esperion Therapeutics, Fibrocor Therapeutics, Poxel Therapeutics, Novo Nordisk and Merck; is a founder and shareholder of Espervita Therapeutics. The remaining authors declare no competing interests.

Appendix A. Supplementary data

Supplementary data to this article can be found online at https://doi.org/10.1016/j.jmccpl.2025.100825.

References

[1] Magliano DJ, Boyko EJ, I.D.F.D.A.t.e.s. committee. IDF Diabetes Atlas. Brussels: International Diabetes Federation ©; 2021.
[2] A.D.A.P.P. Committee. 9. Pharmacologic approaches to glycemic treatment: standards of care in diabetes—2024. Diabetes Care 2023;47(Supplement_1): S158–78.
[3] Boyer JK, Thanigaraj S, Schechtman KB, Pérez JE. Prevalence of ventricular diastolic dysfunction in asymptomatic, normotensive patients with diabetes mellitus. Am J Cardiol 2004;93(7):870–5.
[4] Zabalgoitia M, Ismaeil MF, Anderson L, Maklady FA. Prevalence of diastolic dysfunction in normotensive, asymptomatic patients with well-controlled type 2 diabetes mellitus. Am J Cardiol 2001;87(3):320–3.
[5] Ritchie RH, Abel ED. Basic mechanisms of diabetic heart disease. Circ Res 2020; 126(11):1501–25.
[6] Tan Y, Zhang Z, Zheng C, Wintergerst KA, Keller BB, Cai L. Mechanisms of diabetic cardiomyopathy and potential therapeutic strategies: preclinical and clinical evidence. Nat Rev Cardiol 2020;17(9):585–607.
[7] Packer M. Critical Reanalysis of the Mechanisms Underlying the Cardiorenal Benefits of SGLT2 Inhibitors and Reaffirmation of the Nutrient Deprivation Signaling/Autophagy Hypothesis. Circulation 2022;146(18):1383–405.
[8] Ussher JR, Drucker DJ. Glucagon-like peptide 1 receptor agonists: cardiovascular benefits and mechanisms of action. Nat Rev Cardiol 2023;20(7):463–74.
[9] Almutairi M, Gopal K, Greenwell AA, Young A, Gill R, Aburasayn H, et al. The GLP-1 receptor agonist liraglutide increases myocardial glucose oxidation rates via indirect mechanisms and mitigates experimental diabetic cardiomyopathy. Can J Cardiol 2021;37(1):140–50.
[10] Chan JSF, Greenwell AA, Saed CT, Stenlund MJ, Mangra-Bala IA, Tabatabaei Dakhili SA, et al. Liraglutide alleviates experimental diabetic cardiomyopathy in a PDH-dependent manner. J Endocrinol 2024;262(2).
[11] Sun X, Han F, Lu Q, Li X, Ren D, Zhang J, et al. Empagliflozin ameliorates obesity-related cardiac dysfunction by regulating Sestrin2-mediated AMPK-mTOR

signaling and redox homeostasis in high-fat diet-induced obese mice. Diabetes 2020;69(6):1292–305.
[12] Davies MJ, Aroda VR, Collins BS, Gabbay RA, Green J, Maruthur NM, et al. Management of hyperglycemia in type 2 diabetes, 2022. A consensus report by the American Diabetes Association (ADA) and the European Association for the Study of Diabetes (EASD). Diabetes Care 2022;45(11):2753–86.
[13] Rena G, Hardie DG, Pearson ER. The mechanisms of action of metformin. Diabetologia 2017;60(9):1577–85.
[14] Kasznicki J, Sliwinska A, Drzewoski J. Metformin in cancer prevention and therapy. Ann Transl Med 2014;2(6):57.
[15] Lv Z, Guo Y. Metformin and its benefits for various diseases. Front Endocrinol 2020;11:191.
[16] Han Y, Xie H, Liu Y, Gao P, Yang X, Shen Z. Effect of metformin on all-cause and cardiovascular mortality in patients with coronary artery diseases: a systematic review and an updated meta-analysis. Cardiovasc Diabetol 2019;18(1):96.
[17] Effect of intensive blood-glucose control with metformin on complications in overweight patients with type 2 diabetes (UKPDS 34). UK Prospective Diabetes Study (UKPDS) Group. Lancet 1998;352(9131):854–65.
[18] Hong J, Zhang Y, Lai S, Lv A, Su Q, Dong Y, et al. Effects of metformin versus glipizide on cardiovascular outcomes in patients with type 2 diabetes and coronary artery disease. Diabetes Care 2013;36(5):1304–11.
[19] Xie Z, Lau K, Eby B, Lozano P, He C, Pennington B, et al. Improvement of cardiac functions by chronic metformin treatment is associated with enhanced cardiac autophagy in diabetic OVE26 mice. Diabetes 2011;60(6):1770–8.
[20] Yang Z, Wang M, Zhang Y, Cai F, Jiang B, Zha W, et al. Metformin ameliorates diabetic cardiomyopathy by activating the PK2/PKR pathway. Front Physiol 2020;11:425.
[21] Yang F, Qin Y, Wang Y, Meng S, Xian H, Che H, et al. Metformin inhibits the NLRP3 inflammasome via AMPK/mTOR-dependent effects in diabetic cardiomyopathy. Int J Biol Sci 2019;15(5):1010–9.
[22] Dawood AF, Alzamil NM, Hewett PW, Momenah MA, Dallak M, Kamar SS, et al. Metformin protects against diabetic cardiomyopathy: an association between desmin-sarcomere injury and the iNOS/mTOR/TIMP-1 fibrosis axis. Biomedicines 2022;10(5).
[23] Andersson C, Sogaard P, Hoffmann S, Hansen PR, Vaag A, Major-Pedersen A, et al. Metformin is associated with improved left ventricular diastolic function measured by tissue Doppler imaging in patients with diabetes. Eur J Endocrinol 2010;163(4):593–9.
[24] Ladeiras-Lopes R, Sampaio F, Leite S, Santos-Ferreira D, Vilela E, Leite-Moreira A, et al. Metformin in non-diabetic patients with metabolic syndrome and diastolic dysfunction: the MET-DIME randomized trial. Endocrine 2021;72(3):699–710.
[25] Heather LC, Hafstad AD, Halade GV, Harmancey R, Mellor KM, Mishra PK, et al. Guidelines on models of diabetic heart disease. Am J Physiol Heart Circ Physiol 2022;323(1):H176–200.
[26] Ogawa T, Kouzu H, Osanami A, Tatekoshi Y, Sato T, Kuno A, et al. Downregulation of extramitochondrial BCKDH and its uncoupling from AMP deaminase in type 2 diabetic OLETF rat hearts. Physiol Rep 2023;11(4):e15608.
[27] Day EA, Ford RJ, Smith BK, Mohammadi-Shemirani P, Morrow MR, Gutgesell RM, et al. Metformin-induced increases in GDF15 are important for suppressing appetite and promoting weight loss. Nat Metab 2019;1(12):1202–8.
[28] Chan JSF, Tabatabaei Dakhili SA, Lorenzana-Carrillo MA, Gopal K, Pulente SM, Greenwell AA, et al. Growth differentiation factor 15 alleviates diastolic dysfunction in mice with experimental diabetic cardiomyopathy. Cell Rep 2024;43(8):114573.
[29] Livak KJ, Schmittgen TD. Analysis of relative gene expression data using real-time quantitative PCR and the 2(-Delta Delta C(T)) Method. Methods 2001;25(4):402–8.
[30] Gopal K, Al Batran R, Altamimi TR, Greenwell AA, Saed CT, Tabatabaei Dakhili SA, et al. FoxO1 inhibition alleviates type 2 diabetes-related diastolic dysfunction by increasing myocardial pyruvate dehydrogenase activity. Cell Rep 2021;35(1):108935.
[31] Wu Y. Metformin inhibits mitochondrial dysfunction and apoptosis in cardiomyocytes induced by high glucose via upregulating AMPK activity. Exp Biol Med (Maywood) 2023;248(18):1556–65.
[32] Hawley SA, Gadalla AE, Olsen GS, Hardie DG. The antidiabetic drug metformin activates the AMP-activated protein kinase cascade via an adenine nucleotide-independent mechanism. Diabetes 2002;51(8):2420–5.
[33] Gundewar S, Calvert JW, Jha S, Toedt-Pingel I, Ji SY, Nunez D, et al. Activation of AMP-activated protein kinase by metformin improves left ventricular function and survival in heart failure. Circ Res 2009;104(3):403–11.
[34] Heather LC, Gopal K, Srnic N, Ussher JR. Redefining diabetic cardiomyopathy: perturbations in substrate metabolism at the heart of its pathology. Diabetes 2024;73(5):659–70.
[35] Greenwell AA, Tabatabaei Dakhili SA, Wagg CS, Saed CT, Chan JSF, Yang K, et al. Pharmacological Inhibition of Succinyl Coenzyme A:3-Ketoacid Coenzyme A Transferase Alleviates the Progression of Diabetic Cardiomyopathy. J Am Heart Assoc 2024;13(7):e032697.
[36] Thai PN, Miller CV, King MT, Schaefer S, Veech RL, Chiamvimonvat N, et al. Ketone ester d-β-hydroxybutyrate-(R)-1,3 butanediol prevents decline in cardiac function in type 2 diabetic mice. J Am Heart Assoc 2021;10(19):e020729.
[37] Tong M, Mukai R, Mareedu S, Zhai P, Oka SI, Huang CY, et al. Distinct roles of DRP1 in conventional and alternative mitophagy in obesity cardiomyopathy. Circ Res 2023;133(1):6–21.
[38] Mitra A, Das A, Ghosh S, Sarkar S, Bandyopadhyay D, Gangopadhyay S, et al. Metformin instigates cellular autophagy to ameliorate high-fat diet-induced pancreatic inflammation and fibrosis/EMT in mice. Biochim Biophys Acta Mol Basis Dis 2024;1870(7):167313.
[39] Zhao Y, Sun M. Metformin rescues Parkin protein expression and mitophagy in high glucose-challenged human renal epithelial cells by inhibiting NF-kappaB via PP2A activation. Life Sci 2020;246:117382.
[40] Zhang J, Huang L, Shi X, Yang L, Hua F, Ma J, et al. Metformin protects against myocardial ischemia-reperfusion injury and cell pyroptosis via AMPK/NLRP3 inflammasome pathway. Aging 2020;12(23):24270–87.
[41] Karam HM, Radwan RR. Metformin modulates cardiac endothelial dysfunction, oxidative stress and inflammation in irradiated rats: A new perspective of an antidiabetic drug. Clin Exp Pharmacol Physiol 2019;46(12):1124–32.
[42] Loi H, Kramar S, Laborde C, Marsal D, Pizzinat N, Cussac D, et al. Metformin attenuates postinfarction myocardial fibrosis and inflammation in mice. Int J Mol Sci 2021;22(17).
[43] Regan TJ, Lyons MM, Ahmed SS, Levinson GE, Oldewurtel HA, Ahmad MR, et al. Evidence for cardiomyopathy in familial diabetes mellitus. J Clin Invest 1977;60(4):884–99.
[44] Al-Ani B, Alzamil NM, Hewett PW, Al-Hashem F, Bin-Jaliah I, Shatoor AS, et al. Metformin ameliorates ROS-p53-collagen axis of fibrosis and dyslipidemia in type 2 diabetes mellitus-induced left ventricular injury. Arch Physiol Biochem 2023;129(3):734–40.
[45] Jia W, Bai T, Zeng J, Niu Z, Fan D, Xu X, et al. Combined administration of metformin and atorvastatin attenuates diabetic cardiomyopathy by inhibiting inflammation, apoptosis, and oxidative stress in type 2 diabetic mice. Front Cell Dev Biol 2021;9:634900.
[46] Forcheron F, Basset A, Abdallah P, Del Carmine P, Gadot N, Beylot M. Diabetic cardiomyopathy: effects of fenofibrate and metformin in an experimental model–the Zucker diabetic rat. Cardiovasc Diabetol 2009;8:16.
[47] Steinberg GR, Hardie DG. New insights into activation and function of the AMPK. Nat Rev Mol Cell Biol 2023;24(4):255–72.
[48] Steinberg GR, Kemp BE. AMPK in health and disease. Physiol Rev 2009;89(3):1025–78.
[49] Kim J, Yang G, Kim Y, Kim J, Ha J. AMPK activators: mechanisms of action and physiological activities. Exp Mol Med 2016;48(4):e224.
[50] Coll AP, Chen M, Taskar P, Rimmington D, Patel S, Tadross JA, et al. GDF15 mediates the effects of metformin on body weight and energy balance. Nature 2020;578(7795):444–8.
[51] Qin CX, Sleaby R, Davidoff AJ, Bell JR, De Blasio MJ, Delbridge LM, et al. Insights into the role of maladaptive hexosamine biosynthesis and O-GlcNAcylation in development of diabetic cardiac complications. Pharmacol Res 2017;116:45–56.
[52] Brownlee M, Cerami A, Vlassara H. Advanced glycosylation end products in tissue and the biochemical basis of diabetic complications. N Engl J Med 1988;318(20):1315–21.
[53] Jandeleit-Dahm K, Cooper ME. The role of AGEs in cardiovascular disease. Curr Pharm Des 2008;14(10):979–86.
[54] Wright JN, Collins HE, Wende AR, Chatham JC. O-GlcNAcylation and cardiovascular disease. Biochem Soc Trans 2017;45(2):545–53.
[55] Tikellis C, Thomas MC, Harcourt BE, Coughlan MT, Pete J, Bialkowski K, et al. Cardiac inflammation associated with a Western diet is mediated via activation of RAGE by AGEs. Am J Physiol Endocrinol Metab 2008;295(2):E323–30.
[56] Tate M, Higgins GC, De Blasio MJ, Lindblom R, Prakoso D, Deo M, et al. The mitochondria-targeted methylglyoxal sequestering compound, mitogamide, is cardioprotective in the diabetic heart. Cardiovasc Drugs Ther 2019;33(6):669–74.
[57] Qin L, Wang J, Zhao R, Zhang X, Mei Y. Ginsenoside-Rb1 improved diabetic cardiomyopathy through regulating calcium signaling by alleviating protein O-GlcNAcylation. J Agric Food Chem 2019;67(51):14074–85.
[58] Jyothirmayi GN, Soni BJ, Masurekar M, Lyons M, Regan TJ. Effects of metformin on collagen glycation and diastolic dysfunction in diabetic myocardium. J Cardiovasc Pharmacol Ther 1998;3(4):319–26.
[59] Tang X, Chen XF, Wang NY, Wang XM, Liang ST, Zheng W, et al. SIRT2 acts as a cardioprotective deacetylase in pathological cardiac hypertrophy. Circulation 2017;136(21):2051–67.
[60] Liu Y, Zhang Q, Yang L, Tian W, Yang Y, Xie Y, et al. Metformin attenuates cardiac hypertrophy via the HIF-1α/PPAR-γ signaling pathway in high-fat diet rats. Front Pharmacol 2022;13:919202.
[61] Zhao Q, Song W, Huang J, Wang D, Xu C. Metformin decreased myocardial fibrosis and apoptosis in hyperhomocysteinemia -induced cardiac hypertrophy. Curr Res Transl Med 2021;69(1):103270.
[62] Jiang D, Matsuzaki M, Ida T, Kitamura K, Tsuruda T, Kaikita K, et al. Natriuretic peptides potentiate cardiac hypertrophic response to noradrenaline in rats. Peptides 2023;166:171035.
[63] Foppa M, Duncan BB, Rohde LE. Echocardiography-based left ventricular mass estimation. How should we define hypertrophy? Cardiovasc Ultrasound 2005;3:17.
[64] Fourny N, Beauloye C, Bernard M, Horman S, Desrois M, Bertrand L. Sex differences of the diabetic heart. Front Physiol 2021;12:661297.
[65] Munoz PA, Celermajer DS, Gu Y, Bradley S, Wong J, Constantino MI, et al. Cardiovascular and respiratory measures in adults with early-onset type 2 diabetes mellitus compared with matched controls. Can J Diabetes 2025;49(1):62–69 e1.
[66] Carter RD, Purnama U, Castro-Guarda M, Montes-Aparicio CN, Chandran A, Mbasu R, et al. Systems biology and functional assessments of human iPSC-cardiomyocyte models of insulin resistance capture key hallmarks of diabetic cardiomyopathy. Diabetes 2025;74(11):1929–45.